Gonzalez-Camejo, J.; Barat, R.; Aguado García, D.; Ferrer, J. (2020). Continuous 3-year outdoor operation of a flat-panel membrane photobioreactor to treat effluent from an anaerobic membrane bioreactor. Water Research. 169:1-12. https://doi.org/10.1016/j.watres.2019.115238

Continuous 3-year outdoor operation of a flat-panel membrane photobioreactor to treat effluent from an anaerobic membrane bioreactor

J. González-Camejo*, R. Barat, D. Aguado, J. Ferrer.

CALAGUA – Unidad Mixta UV-UPV, Institut Universitari d'Investigació d'Enginyeria de l'Aigua i Medi Ambient – IIAMA, Universitat Politècnica de València, Camí de Vera s/n, 46022 Valencia, Spain

*Corresponding author: jogonca4@upv.es

Abstract

A membrane photobioreactor (MPBR) plant was operated continuously for 3 years to evaluate the separate effects of different factors, including: biomass and hydraulic retention times (BRT, HRT), light path (Lp), nitrification rate (NOxR), nutrient loading rates (NLR, PLR) and others. The overall effect of all these parameters, which influence MPBR performance had not previously been assessed. The multivariate projection approach chosen for this study provided a good description of the collected data and facilitated their visualisation and interpretation.

Forty variables used to control and assess MPBR performance were evaluated during three years of continuous outdoor operation by means of principal component analysis (PCA) and partial least squares (PLS) analysis. The PCA identified the photobioreactor light path as the factor with the largest influence on data variability. Other important factors were: nitrogen and phosphorus recovery rates (NRR, PRR), biomass productivity (BP), optical density of 680 nm (OD680), ammonium and phosphorus effluent concentration (NH_4, P), HRT, BRT, air flow rate (F_{air}) and nitrogen and phosphorus loading rates (NLR and PLR). The MPBR performance could be adequately estimated by a PLS model based on all the recorded variables, but this estimation

worsened appreciably when only the controlled variables (Lp, F_{air}, HRT and BRT) were used as predictors, which underlines the importance of the non-controlled variables on MPBR performance. The microalgae cultivation process could thus only be partially controlled by the design and operating variables.

A high nitrification rate was found to be inadvisable, since it showed an inverse correlation with NRR. In this respect, temperature and microalgae biomass concentration appeared to be the main factors to mitigate nitrifying bacteria activity.

Keywords: Membrane photobioreactor; microalgae; nitrifying bacteria; PCA; PLS; outdoor.

1 Introduction

The ever-increasing population together with human activities are the main factors responsible for the recent growth in wastewater production (Ling *et al.,* 2019). To avoid serious pollution problems, wastewater effluents must be properly treated prior to their discharge into natural water bodies (Song *et al.*, 2018). Although urban wastewater treatment plants (WWTPs) are now extremely efficient as regards removing pollutants, they consume huge amounts of energy (Ling *et al*., 2019; Marazzi *et al.*, 2019) and the nutrients are usually lost by nitrogen stripping or phosphorus precipitation (Whitton *et al.*, 2016).

The wastewater treatment sector thus needs to intensify research on more sustainable technologies, not only to remove pollutants from wastewater but also to recover resources from them, mainly energy, nutrients and reclaimed water (Nayak *et al*., 2018; Seco *et al.*, 2018).

Anaerobic membrane bioreactors (AnMBRs) have been attracting much attention since they present lower energy consumption, sludge production and space requirements than the classical aerobic processes (Robles *et al.*, 2013). They can also produce biogas from organic matter that can sometimes offset the energy required for the treatment process (Song *et al.*, 2018).

AnMBR systems have previously been assessed on a pilot scale, obtaining a high quality effluent as regards organic matter and suspended solids (Seco *et al.*, 2018). However, their direct discharge into sensitive water bodies is not permitted, since these systems contain a large amount of nutrients (Song *et al.*, 2018) which can lead to eutrophication, i.e. the sudden proliferation of algae in natural waters, which reduces water quality, increases health risks and impairs wildlife (Lau *et al.*, 2019). Microalgae cultivation has emerged as the ideal option to avoid this problem, as it can recover nutrients from AnMBR effluents (González-Camejo *et al.*, 2019a). It also produces valuable microalgae biomass that can be used to obtain biofuels or fertilisers, amongst other applications (Seco *et al.*, 2018; Xu *et al.*, 2019).

Microalgae can be cultivated in either open ponds or closed photobioreactors (PBRs) (Nwoba *et al.*, 2019). The latter is able to achieve higher biomass production and recover more nutrients than open reactors. However, very few of these plants are being operated at industrial scale, mainly due to the inefficiency of large-scale cultivation techniques (Kubelka *et al.*, 2018; Nayak *et al.*, 2018; Xu *et al.*, 2019). It therefore seems essential to obtain experimental data from real sewage plants for the implementation of large-scale outdoor microalgae-based wastewater systems.

Microalgae cultivation is a high complex process which concerns mass, heat and light transfer as well as biological reactions (Xu *et al.*, 2019). Several authors have reported seasonal variations in the performance of outdoor microalgae systems (García *et al.*,

2018). Apart from ambient conditions (mainly solar light and temperature), there are many other factors that influence microalgae growth: PBR design, mixing rate, nutrient loading rates, microalgae strains, biomass and hydraulic retention time (BRT, HRT), competition with other microorganisms, inhibition by toxic substances, etc. (Cho *et al.*, 2019; Marazzi *et al.*, 2019). Some of these factors have been independently evaluated in outdoor flat-panel MPBRs in previous studies (Table 1). As can be seen, MPBR performance varies widely, with nitrogen recovery rates ranging from 1.9 mg $N \cdot L^{-1} \cdot d^{-1}$ when the plant was operated as a PBR system (i.e. without filtration) to 21.1 mg $N \cdot L^{-1} \cdot d^{-1}$ when MPBR operations were based on the optimal design and control parameters. It therefore seems to be worth analysing thoroughly all the recorded variables simultaneously to identify any possible relationships with process performance and to gain valuable in-depth knowledge on the process.

Table 1. Summary of the results obtained in previous studies

Parameter evaluated	Value	Results			Reference
		NRR	PRR	BP	
	20 mg $S \cdot L^{-1}$	6.0	1.3	79	
Microalgae-AOB competition	ATU = 0 mg$\cdot L^{-1}$	1.9	0.2	27	González-Camejo *et al.*, 2018*
	ATU = 5 mg$\cdot L^{-1}$	2.3	0.3	19	
NLR/PLR	9.7/1.3 g$\cdot d^{-1}$	12.5	1.5	72	González-Camejo *et al.*, 2018
	14.4/1.8 g$\cdot d^{-1}$	11.5	1.4	69	
	8.4/1.1 g$\cdot d^{-1}$	7.5	1.1	78	
BRT	4.5 d	10.3	1.1	74	González-Camejo *et al.*, 2019a
	6 d	9.9	1.2	74	
	9 d	7.6	1.0	65	
HRT	3.5 d	11.1	1.4	65	González-Camejo *et al.*, 2019a
	2 d	9.3	1.1	65	
	1 d	8.7	1.4	54	
Light path	25 cm	9.1	1.2	66	González-Camejo *et al.*, 2019a; 2019b
	10 cm	19.4	2.2	152	
NO_2 inhibition	BRT = 2 d[1]	14.1	13.5[3]	136	González-Camejo *et al.*, 2019b
	BRT = 2.5 d[2]	19.4	12.0[3]	152	
	BRT = 4.5 d[2]	14.5	24.3[3]	108	

*NRR: nitrogen recovery rate (mg $N \cdot L^{-1} \cdot d^{-1}$); PRR: phosphorus recovery rate (mg $P \cdot L^{-1} \cdot d^{-1}$); BP: biomass productivity (mg $VSS \cdot L^{-1} \cdot d^{-1}$); H_2S: sulphide; ATU: allylthiourea to inhibit nitrification; NLR: nitrogen loading rate; PLR: phosphorus loading rate; BRT: biomass retention time; HRT: hydraulic retention time. *Operation in a PBR system (without filtration): not considered for PCA and PLS; [1]Significant presence of nitrite in the culture; [2]Negligible NO_2 concentration in the culture; [3]Values of nitrification rate (mg $N \cdot L^{-1} \cdot d^{-1}$).*

PCA and PLS have been shown to be useful for understanding processes and optimising the performance of WWTPs based on activated sludge technology (Han *et al.*, 2018). Trials have also been carried out recently on optimising the microalgae cultivation conditions of multiple variables using statistical methods on lab-scale data (Nayak *et al.*, 2018). Viruela *et al.* (2018) also used these multivariate techniques to assess the relationship between microalgae performance (in terms of nutrient recovery and biomass productivity) with light, temperature and N:P ratio in the short-term (around 4-5 months) operation of an outdoor MPBR.

The availability of real long-term data under outdoor conditions is very limited, and is especially scarce for periods longer than 12 months. The present study evaluates the three-year operation of an outdoor flat-panel MPBR plant, considering all the relevant variables, from which valuable information could be obtained on the behaviour of microalgae cultures in different ambient and operating conditions.

The competition between microalgae-nitrifying bacteria for ammonium uptake has been identified as a highly relevant factor in the performance of a mixed microalgae culture (Galès *et al.*, 2019; González-Camejo *et al.*, 2019c), so that determining the most important parameters in nitrifying bacteria activity would help to maintain bacteria growth at a minimum and favour microalgae growth.

The aim of this study was therefore to use multivariate projection techniques to analyse the data collected from operating an outdoor MPBR plant treating AnMBR effluent for three years in order to identify the key variables in the process and any relationships between the parameters.

2 Material and methods

2.1 Microalgae and wastewater

The nutrient-rich influent to the MPBR plant was from an AnMBR plant that treated real sewage (details of this plant and its operation can be found in Seco *et al.* (2018)). The average characteristics of the substrate were a chemical oxygen demand (COD) concentration of 67 ± 7 mg $COD \cdot L^{-1}$, a nitrogen concentration of 52.4 ± 8.8 mg $N \cdot L^{-1}$ (mainly in the form of ammonium (NH_4 > 95%), with low amounts of nitrite (NO_2) and nitrate (NO_3)), and a phosphorus concentration of 5.7 ± 1.5 mg $P \cdot L^{-1}$ as phosphate (PO_4). The considerable variability of the influent characteristics was due to changes in both sewage composition and AnMBR plant performance.

Microalgae were originally obtained from the walls of the secondary settler at the Carraixet WWTP and mainly consisted of a mixed culture of the eukaryotic microalgae genera *Chlorella* and *Scenedesmus*, although low concentrations of cyanobacteria, nitrifying and heterotrophic bacteria were also present.

2.2 MPBR plant

The MPBR pilot plant was in the Carraixet WWTP (39º30’04.0’’N 0º20’00.1’’W, Valencia, Spain) and operated continuously outdoors from June 2015 to May 2018. During the experimental period the hydraulic retention time (HRT) varied in the range of 1-3.5 d, while biomass retention time (BRT) was between 2-9 d. However, there were several periods in which operations were stopped for maintenance and there were also periods in batch mode, which were not considered for the evaluation of the MPBR operations.

The MPBR plant consisted of two flat-panel PBRs which discharged the culture to a membrane tank (MT) to separate the microalgae biomass from the permeate. Full

description of the MPBR plant operation can be found in González-Camejo *et al.* (2019a). Both PBRs were continuously air-stirred to ensure appropriate mixing to homogenise the culture in terms of nutrient concentration, temperature and light availability. It also reduced wall fouling and avoided microalgae settling. An on-off valve was opened for 5 s to introduce pure pressurised CO_2 (99.9%) into the air system whenever the pH measurements rose over 7.5 to maintain optimum pH (Qiu *et al.*, 2017) and ensure carbon-replete conditions. Twelve LED lamps (Unique Led IP65 WS-TP4S-40W-ME) were installed on the rear wall of the PBRs to apply a continuous irradiance of 300 $\mu mol \cdot m^{-2} \cdot s^{-1}$. The culture was cooled by a thermostatically controlled system (Daikin Inverter R410A). The temperature set-point was 25 ºC to keep temperatures below 30 ºC, avoiding culture deterioration (González-Camejo *et al.*, 2019c).

Two different MPBR plants were operated: i) one with a 25-cm light path PBRs (550 L each) during the first half of the operation; i.e., from June 2015 until December 2016; and ii) another with a 10-cm light path PBRs (230 L each): from January 2017 until the end of the operating period.

The MT had a filtering area of 3.4 m^2 and included an industrial hollow-fibre ultrafiltration membrane unit (PURON® Koch Membrane Systems model PUR-PSH31, 0.03 μm pore size). Its total volume accounted for 14 L, which meant non-photic volume of 1.25% for the 25-cm MPBR plant and 2.9% for the 10-cm MPBR plant. The MT was stirred by the same airflow as the PBRs. Membrane operation consisted of a combination of 250 s filtration and 50 s relaxation (F-R cycle) (Robles *et al.,* 2013). 40 s of back-flushing (in which permeate was introduced into the MT to strip fouling out of the membrane) were performed every 10 F–R cycles. Moreover, 60 s of ventilation every 20 F–R cycles and 60 s of degasification every 50 F–R cycles were carried out. In

the ventilation stage, permeate is pumped from the top of the MT instead of being introduced through the membrane pores (as in back-flushing). With respect to degasification stage, it consists of a high flow rate filtration period with the goal of removing the accumulated gas on the top of the fibres. The gross 20 ºC-standardised transmembrane flux (J_{20}) was kept in the range of 15-30 LMH ($L \cdot m^{-2} \cdot s^{-1}$). The average specific gas demand per unit of membrane area (SGDm) was kept around 0.3-0.4 $Nm^3 \cdot h^{-1} \cdot m^{-2}$. The filtration process was operated continuously, but only the corresponding amount of permeate was extracted to control HRT, recycling to the system the rest of permeate that was not taken out of the MPBR plant.

2.3 Sampling and Analytical Methods

During the continuous operations, grab samples were collected in duplicate three times a week from the MBPR influent (AnMBR effluent after aeration) and effluent (permeate from the filtration unit) as well as from the MPBR culture; i.e. treated water plus suspended solids. Ammonium, nitrite, nitrate and phosphate, volatile suspended solids (VSS), total chemical oxygen demand (COD), soluble chemical oxygen demand (sCOD), total nitrogen and total phosphorus in the culture were analysed according to Standard Methods (APHA, 2005). Nutrient concentrations were measured by an automatic analyser (Smartchem 200, Westco Scientific Instruments, Westco). COD, sCOD, total nitrogen and phosphorus were measured in duplicate once a week.

Optical density at 680 nm (OD680) and maximum quantum yield of photosystem II (F_v/F_m) were measured in-situ by a portable fluorometer AquaPen-C AP-C 100 (Photon Systems Instruments). To measure F_v/F_m, the samples were kept in the dark for ten minutes to become dark-adapted.

Total eukaryotic cells (TEC) were counted twice a week by epifluorescence microscopy on a Leica DM2500 with a 100x-oil immersion lens. A minimum of 300 cells were counted in duplicate plus at least 100 cells of the most abundant genera with an error of less than 20%.

2.4 Calculations

Biomass productivity (mg VSS·L^{-1}·d^{-1}), nitrogen recovery rate (NRR) (mg N·L^{-1}·d^{-1}) and phosphorus recovery rate (PRR) (mg P·L^{-1}·d^{-1}) were calculated following González-Camejo *et al.* (2018).

I_{av} was calculated by applying the Lambert-Beer Law (Eq. 1) as reported by Romero-Villegas *et al.* (2018):

$$I_{av} = \frac{tPAR}{K_a \cdot C_b \cdot Lp} \cdot (1 - e^{-K_a \cdot C_b \cdot Lp}) \qquad \text{(Eq. 1)}$$

Where tPAR is the sum of the solar and artificial photosynthetically active radiation applied to the PBRs (µmol·m^{-2}·s^{-1}), K_a is an extinction coefficient (m^2·g^{-1}, Eq. 2), C_b is the culture biomass concentration (g·m^{-3}), and Lp is the light path (m).

$$K_a = \frac{OD_{400-700}}{C_b \cdot Lp_c} \qquad \text{(Eq. 2)}$$

where $OD_{400\text{-}700}$ (-) is the average optical density of the culture in the range of 400-700 nm; and Lp_c (m) is the light path of the spectrophotometer´s cuvette.

The nitrification rate (NOxR) (mg N·L^{-1}·d^{-1}) was obtained by Eq. 3:

$$\text{NOxR} = \frac{F \cdot (NOx_e - NOx_i)}{V_{MPBR}} \qquad \text{(Eq. 3)}$$

where F is the treatment flow rate (m^3·d^{-1}); NOx_e the concentration of nitrite plus nitrate from the effluent (mg N·L^{-1}); NO_{xi} is the concentration of nitrite plus nitrate from the influent (mg N·L^{-1}); and V_{MPBR} is the volume of culture in the MPBR plant (m^3). It

should be remembered that negative NOxR values indicate that the microalgae NO_x uptake is higher than the NOx produced by the nitrifiers.

2.5 Statistical analysis

2.5.1 Principal component analysis

PCA was conducted to assess the relationship between different ambient, operating, design and cultivation conditions on the performance of the outdoor MPBR plant. This multivariate technique enables to visualise the correlation structure between the variables as well as identify patterns in the data such as trends and anomalous data. Principal components (PC) are obtained by linear combination of the original variables, capturing the underlying phenomenon in the studied system.

The matrix analysed consisted of 40 variables measured in 560 samples (observations). The variables considered included controllable, ambient, influent, effluent, culture and performance variables (Table 2). The ambient parameters; i.e. solar photosynthetically active radiation (PAR) and culture temperature (T) were monitored since they have been widely reported as the main factors in microalgae growth (García *et al.*, 2018; Viruela *et al.*, 2018). These parameters represent the daily average obtained from all the monitored values (each of them recorded every 10 seconds). The maximum (PAR_{max}, T_{max}) and minimum (T_{min}) daily values of these parameters were also considered as their fluctuations can significantly influence microalgae performance (Ippoliti *et al.*, 2016). Light path (Lp), HRT, BRT and air flow rate (F_{air}) were the only parameters which could be modified and were thus labelled as controllable variables. Dissolved oxygen (DO) concentration has also been reported as a key factor in microalgae performance (Ippoliti *et al*., 2016), as have the nutrient loading rates (González-Camejo *et al*., 2018), i.e. nitrogen (NLR) and phosphorus loading rates (PLR). NRR, PRR, and BP were

included since they have been widely used to assess the performance of microalgae cultivation systems (Marazzi *et al.*, 2019). Other parameters such as average light irradiance (I_{av}), maximum quantum efficiency (F_v/F_m) and optical density at 680 nm (OD680) can provide information on the use of light in the culture, which is related to the efficiency of the system (Romero-Villegas *et al.*, 2018). As the main goal of the MPBR plant is to treat AnMBR effluent, the effluent nutrient concentrations are obviously relevant parameters (García *et al.*, 2018) and can serve as indicators of the treatment process. Total eukaryotic cell (TEC) concentration, as well as the concentration of genera *Scenedesmus* (Sc) and *Chlorella* (Chl), were also included to evaluate the possible shift in the microalgae population caused by external factors. COD was measured to assess the effect of microalgae stress on MPBR performance (Lau *et al.*, 2019; Lee *et al.*, 2018). Optical density ratio between 680 and 750 nm (OD680:OD750) has been reported to be related to the microalgae chlorophyll content (Markou *et al.*, 2017) and was therefore analysed. pH was also included as the microalgae activity modifies pH and in turn is affected by it (Qiu *et al.*, 2017). Lastly, since the competition between microalgae and ammonium oxidising bacteria (AOB) can be significant when treating AnMBR effluents (González-Camejo *et al.*, 2019c), nitrification rate (NOxR) was also considered as indicator of the nitrification process in the system. Table 2 shows all the variables used in the PCA and their abbreviations, as well as their average values.

Table 2. Variables used in the PCA

	Acronym	Variable	Unit	Average value (mean ± SD)
Controlled variables	BRT	Biomass retention time	d	4.3 ± 1.6
	HRT	Hydraulic retention time	d	1.8 ± 0.7
	Lp	PBR light path	cm	25/10
	F_{air}	Air flow rate	vvm	0.14 ± 0.07

	Acronym	Variable	Unit	Average value (mean ± SD)
Ambient variables	PAR	Daily average PAR	$\mu mol \cdot m^{-2} \cdot s^{-1}$	273 ± 102
	PAR_{max}	Daily maximum PAR	$\mu mol \cdot m^{-2} \cdot s^{-1}$	1298 ± 380
	T	Temperature	ºC	23.1 ± 3.3
	T_{max}	Maximum temperature	ºC	26.7 ± 3.4
	T_{min}	Minimum temperature	ºC	20.0 ± 4.0
Influent variables	NLR	Nitrogen loading rate	$g\ N \cdot d^{-1}$	22.0 ± 9.7
	PLR	Phosphorus loading rate	$g\ P \cdot d^{-1}$	2.4 ± 1.5
	$N:P_i$	Nitrogen-phosphorus ratio of the influent	molar	26.3 ± 13.9
	COD_i	Total chemical oxygen demand of the influent	$mg\ COD \cdot L^{-1}$	65 ± 29
Culture variables	VSS	Volatile suspended solids	$mg\ VSS \cdot L^{-1}$	509 ± 229
	OD_{680}	Optical density at 680 nm	-	0.71 ± 0.37
	$OD_{680}:OD_{750}$	Optical density ratio between 680 and 750 nm	-	1.11 ± 0.03
	pH	pH	-	7.4 ± 0.3
	F_v/F_m	Maximum quantum efficiency	-	0.67 ± 0.06
	DO	Dissolved oxygen	$mg\ O_2 \cdot L^{-1}$	11.0 ± 1.3
	DO_{max}	Maximum dissolved oxygen	$mg\ O_2 \cdot L^{-1}$	14.0 ± 2.2
	DO_{min}	Minimum dissolved oxygen	$mg\ O_2 \cdot L^{-1}$	8.9 ± 0.7
	COD	Total chemical oxygen demand of the culture	$mg\ COD \cdot L^{-1}$	1087 ± 458
	sCOD	Soluble chemical oxygen demand of the culture	$mg\ COD \cdot L^{-1}$	139 ± 71
	N_i	Intracellular nitrogen content	%	8.0 ± 2.5
	P_i	Intracellular phosphorus content	%	1.1 ± 0.3
	$N:P_b$	Nitrogen-phosphorus ratio of the biomass	molar	16.7 ± 7.4
	TEC	Total eukaryotic cell concentration	$cells \cdot L^{-1}$	$1.64 \cdot 10^{10} \pm 1.23 \cdot 10^{10}$
	Chl	*Chlorella* concentration	$cells \cdot L^{-1}$	$1.46 \cdot 10^{10} \pm 1.39 \cdot 10^{10}$
	Sc	*Scenedesmus* concentration	$cells \cdot L^{-1}$	$1.75 \cdot 10^{9} \pm 2.39 \cdot 10^{9}$
	I_{av}	Average light irradiance in the PBR	$\mu mol \cdot m^{-2} \cdot s^{-1}$	39.0 ± 17.7
	NO_xR	Nitrification rate	$mg\ N \cdot L^{-1} \cdot d^{-1}$	8.8 ± 9.5
Effluent variables	NH_4	Ammonium effluent concentration	$mg\ N \cdot L^{-1}$	19.5 ± 15.2
	NO_2	Nitrite effluent concentration	$mg\ N \cdot L^{-1}$	0.6 ± 1.7
	NO_3	Nitrate effluent concentration	$mg\ N \cdot L^{-1}$	5.5 ± 8.8
	N_t	Total nitrogen effluent concentration	$mg\ N \cdot L^{-1}$	25.6 ± 13.1
	P	Phosphorus effluent concentration	$mg\ P \cdot L^{-1}$	2.3 ± 1.9
	COD_e	Total chemical oxygen demand of the effluent	$mg\ COD \cdot L^{-1}$	41 ± 19
Performance variables	NRR	Nitrogen recovery rate	$mg\ N \cdot L^{-1} \cdot d^{-1}$	16.0 ± 8.2
	PRR	Phosphorus recovery rate	$mg\ P \cdot L^{-1} \cdot d^{-1}$	1.9 ± 1.1
	BP	Biomass productivity	$mg\ VSS \cdot L^{-1} \cdot d^{-1}$	130 ± 77

PAR: Photosynthetically active radiation

It should be noted that all the variables shown in Table 2 were related to the MPBR biological process and parameters related to membrane filtration were not considered in the statistical analysis.

2.5.2 Partial Least Squares analysis

PLS is a multivariate projection technique that uses two different groups of data; i.e. predictors (X) and responses (Y). Its goal is to find latent variables that are not only able to explain the variance in X, but also the variance which best predicts the Y variables.

To identify the variables with the strongest possible relationship with process performance, PLS analysis was used with NRR, PRR and BP as responses (Y), while all the other variables used in the PCA were predictors (X). Effluent variables were included as predictors (in spite of also being a result of the process) because NO_2 and NO_3 are related to nitrification (González-Camejo *et al.,* 2018), while NH_4, N_t and P can also be indicators of nutrient limitation (Pachés *et al.* 2018).

Since the competition between microalgae and nitrifying bacteria can seriously affect MPBR performance (González-Camejo *et al.*, 2019c), a further PLS analysis was carried out with the nitrification rate (NOxR) as the response and all the other variables as predictors (X). Performance variables were also used as predictors as some authors have suggested lower nitrification when microalgae activity is high (González-Camejo *et al.*, 2019b; Rada-Ariza e*t al.*, 2019).

Both PCA and PLS were conducted on SIMCA-P 10.0 software (Umetrics, Umea, Sweden).

3 Results and discussion

Figure 1 shows the evolution of the main performance parameters (NRR, PRR and BP) during the 3-year period of MPBR operations. As can be seen in this figure, all three variables varied widely. It should be highlighted that the evident improvement in MPBR performance after December 2016 corresponded to the reduction of the MPBR light path from 25 to 10 cm. Since the aim of the MPBR was to treat AnMBR effluent, it also has to be noted that the legal discharge limits (i.e., 15 mg $N \cdot L^{-1}$ and 2 mg $P \cdot L^{-1}$ according to European Directive 91/271/CEE for a 10,000-100,000-p.e WWTP) were only reached between May-December 2017 (data not shown), which coincides with the highest MPBR performance (Figure 1). It therefore seems essential to determine the conditions that make it possible to meet these limits for the proper treatment of AnMBR effluents.

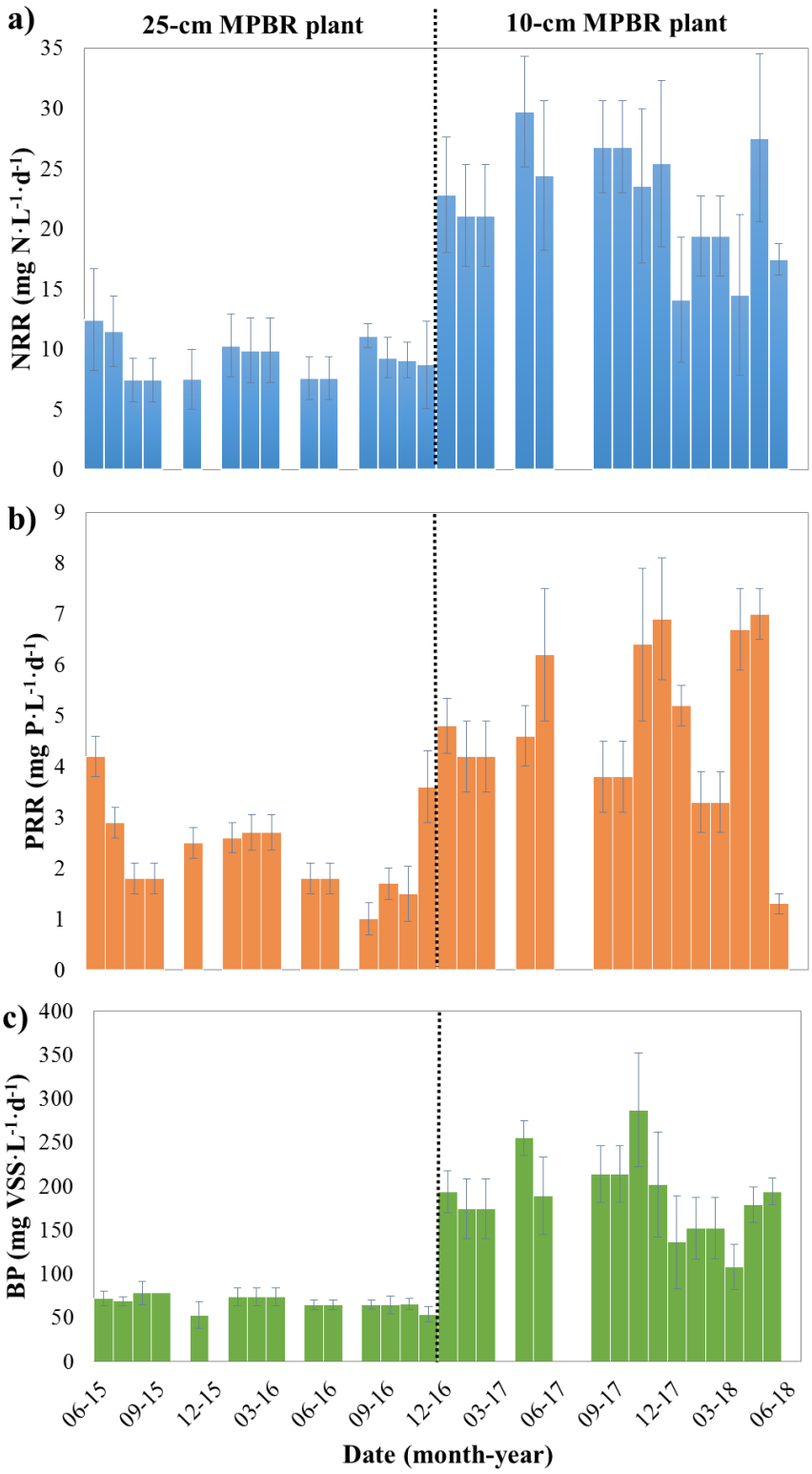

Figure 1. *MPBR Performance along the 3-year operating period: a) Nitrogen recovery rates (NRR); a) phosphorus recovery rates (PRR); and c) biomass productivity (BP).*

3.1 Principal component analysis

Raw data was mean-centred and scaled to unit variance to give equal importance to each of the variables in the multivariate projection models. A PCA model was fitted to the pre-processed data. Four statistically significant principal components (PC) were found, according to the cross-validation of the model, explaining 63.9% of the total variance (34.6%, 13.8%, 8.0% and 7.5% for PC1, PC2, PC3 and PC4, respectively). This explained variance value is high enough to consider that the PCA model gave a fairly accurate description of the real data from the MPBR plant.

Figure 2 shows the main results of the PCA model (score and loading plots).

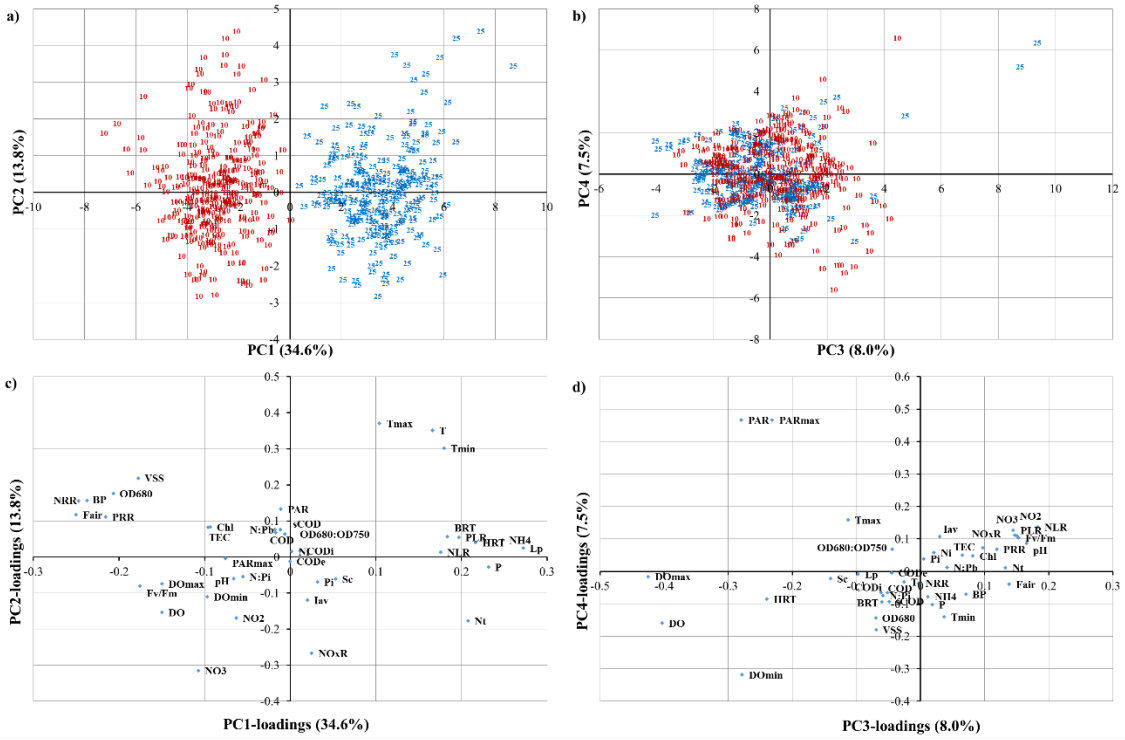

Figure 2. *PCA-score plots showing the distribution of observations:* ***a)*** *PC1 vs PC2;* ***b)*** *PC3 vs PC4; PCA-loading plot showing the correlation pattern between variables:* ***c)*** *PC1 vs PC2;* ***d)*** *PC3 vs PC4.*

In Figure 2a (score plot of the two first components), a markedly different behaviour can be observed with respect to PC1 (which explains most of the data variability; i.e., 34.6%) in the samples collected from the 10-cm MPBR plant (red points), which are on the left of the graph; and the samples from the 25-cm MPBR plant (blue points) on the right. This separation between samples is due to the variables with higher weight in PC1, which were significantly different in each MPBR plant.

Figure 2c shows the correlation patterns of all the variables. The positively correlated variables are grouped together in the same quadrant, while those inversely correlated can be seen on opposite sides of the plot origin (i.e. in the diagonally opposed quadrants). Note that the distance of a given variable from the plot origin shows the impact of each variable on the model (the longer the distance the stronger the impact). Apart from Lp, which was obviously different in each MPBR (due to the shift in PBR width), variations in NLR and PLR (nutrient loads), as well as in F_{air}, were highly influenced by the reduction of MPBR volume. In addition, BRT and HRT ranges differed in each MPBR plant; i.e. 4.5-9-d BRT and 1-3.5-d HRT for the 25-cm MPBR plant and 2-4.5-d BRT and 1-1.5-d HRT for the 10-cm MPBR plant. Performance variables (NRR, PRR and BP) were also very different in each MPBR (as can be observed in Figure 1). It must be noted that these clear differences in MPBR performance in each MPBR plant are likely related to light distribution along the PBRs since light availability is reduced at a higher light path (Cho *et al.*, 2019). Probably for this reason light path was the parameter with the highest weight in PC1 (0.272, see Figure 2c). Moreover, the decline in MPBR performance entailed higher effluent nutrient concentrations. This implied that NH_4, N_t and P showed significantly different values and were inversely related to the performance variables (Figure 2c). With respect to nutrient loading rates, high correlation between NLR and PLR and effluent nutrient

concentrations was observed (Figure 2c). Other studies have reported effluent concentrations to directly depend on nutrient loads in non-nutrient-limited systems (Arbib *et al.*, 2013; González-Camejo *et al.*, 2018). In this respect, the MPBR plant was not nutrient-limited during most of the 3-year operation (data not shown). The dependence of effluent nutrient concentrations with nutrient loading rates makes effluent concentration values barely comparable with different sub-periods or with other cultivation systems. For this reason, microalgae performance was assessed in terms of biomass productivity and nutrient recovery rates instead.

On the other hand, solar PAR and oxygen concentration, which have been reported to be highly relevant in microalgae cultivation systems (Ippoliti *et al.*, 2016; Moreno-García *et al.*, 2019; Viruela *et al.*, 2018), were relevant in PC3 and PC4 (Figure 2d, 15.5% of total variance) but not in the first two components: PC1 and PC2 (48.4% of total variance, see Figure 2c).

Since performance variables (i.e. NRR, PRR and BP) seemed to be highly related in the PCA (Figure 2c), lineal correlations between them were carried out (Figure 3). Results showed that all these performance variables were statistically related (p-value < 0.01). However, data was dispersed, showing coefficients of determination (R^2) of 59.8%, 66.8% and 42.8% for relations NRR-PRR, NRR-BP and PRR-BP, respectively (Figure 3). It has to be highlighted that PRR showed the lowest correlation because phosphorus uptake also depends on internal phosphorus (Powell *et al.*, 2009). Despite the correlation between NRR and BP was higher than those for phosphorus, its relatively low R^2-coefficient value was probably due to NRR being more dependent on light intensity (which can be very variable from one day to another); while BP is hardly dependent on temperature, which variations are slower than those of light (Viruela *et al.*, 2018).

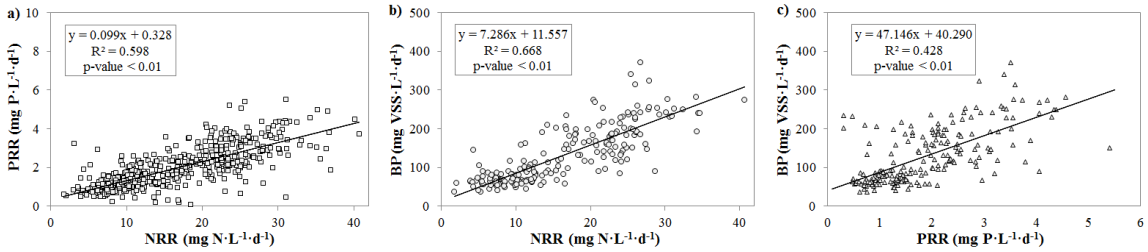

Figure 3. *Linear correlations between performance variables:* ***a)*** *Nitrogen recovery rate (NRR)* ***)*** *vs Phosphorus recovery rate (PRR);* ***b)*** *NRR vs Biomass productivity (BP); and* ***c)*** *PRR vs BP.*

In addition, some culture performance appeared to be highly related in the PCA. For instance, OD680 and VSS were close to each other in the PCA-loading plot (Figure 2c). Linear correlation between these variables corroborated this relationship, showing a high R^2-coefficient of 90.5% (Figure 4a), similar to what has been reported by other authors (Ling *et al.*, 2019). The high correlation between this optical parameter and VSS thus suggested that the culture biomass was mainly composed by microalgae since OD680 is related to the chlorophyll content of microalgae (Markou *et al.*, 2017). In fact, OD680 and VSS were also highly correlated to TEC (Figure 4b, 4c). Specifically, most of these eukaryotic microalgae cell corresponded to genus *Chlorella* (Chl) (Figure 4d), as shown by the average percentage of *Chlorella* with respect to TEC, which accounted for 65.0 ± 39.6% during the 3-year operation.

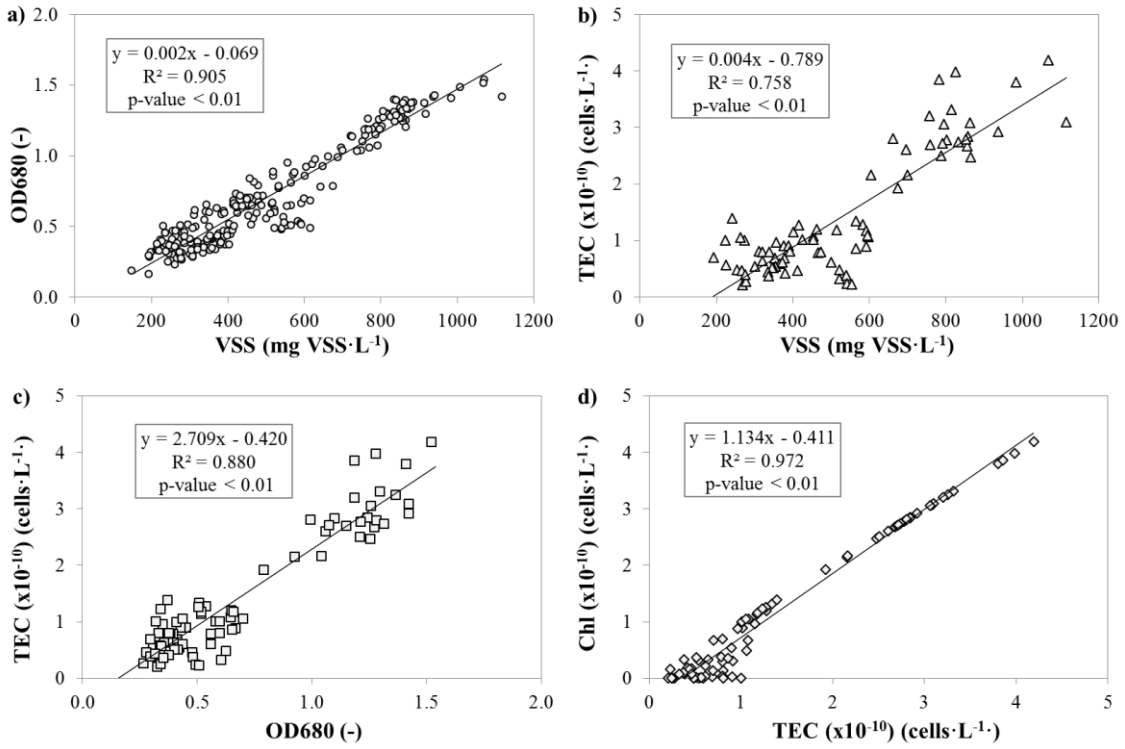

Figure 4. *Linear correlations between culture variables:* ***a)*** *Volatile suspended solids (VSS)* ***b)*** *vs optical density of 680 nm (OD680);* ***b)*** *VSS vs total eukaryotic cells (TEC);* ***c)*** *OD680 vs TEC; and* ***c)*** *TEC vs Chlorella (Chl).*

3.2 PLS analysis

A PLS analysis was carried out to predict the parameters related to MPBR performance (i.e., NRR, PRR and BP), which were used as responses, while all the remaining variables were predictors. Four latent variables were statistically significant, according to cross-validation. The model was well balanced between fit and prediction performance, explaining 55.5% (R^2_x) of the X-matrix (matrix of predictors) variance and an accumulated explained variance of the response matrix (Y) of 75.6% (R^2_y). Goodness of prediction (Q^2) accounted for 71.6%.

Figures 5a, 5b and 5c display the recorded values of NRR, PRR and BP versus the PLS predicted values, evidencing the good fit obtained for the three MPBR performance variables. The prediction was especially good for biomass productivity (R^2= 0.920), as

could be expected due to the high positive correlation in the PLS model between OD680 and VSS (Figure 6a).

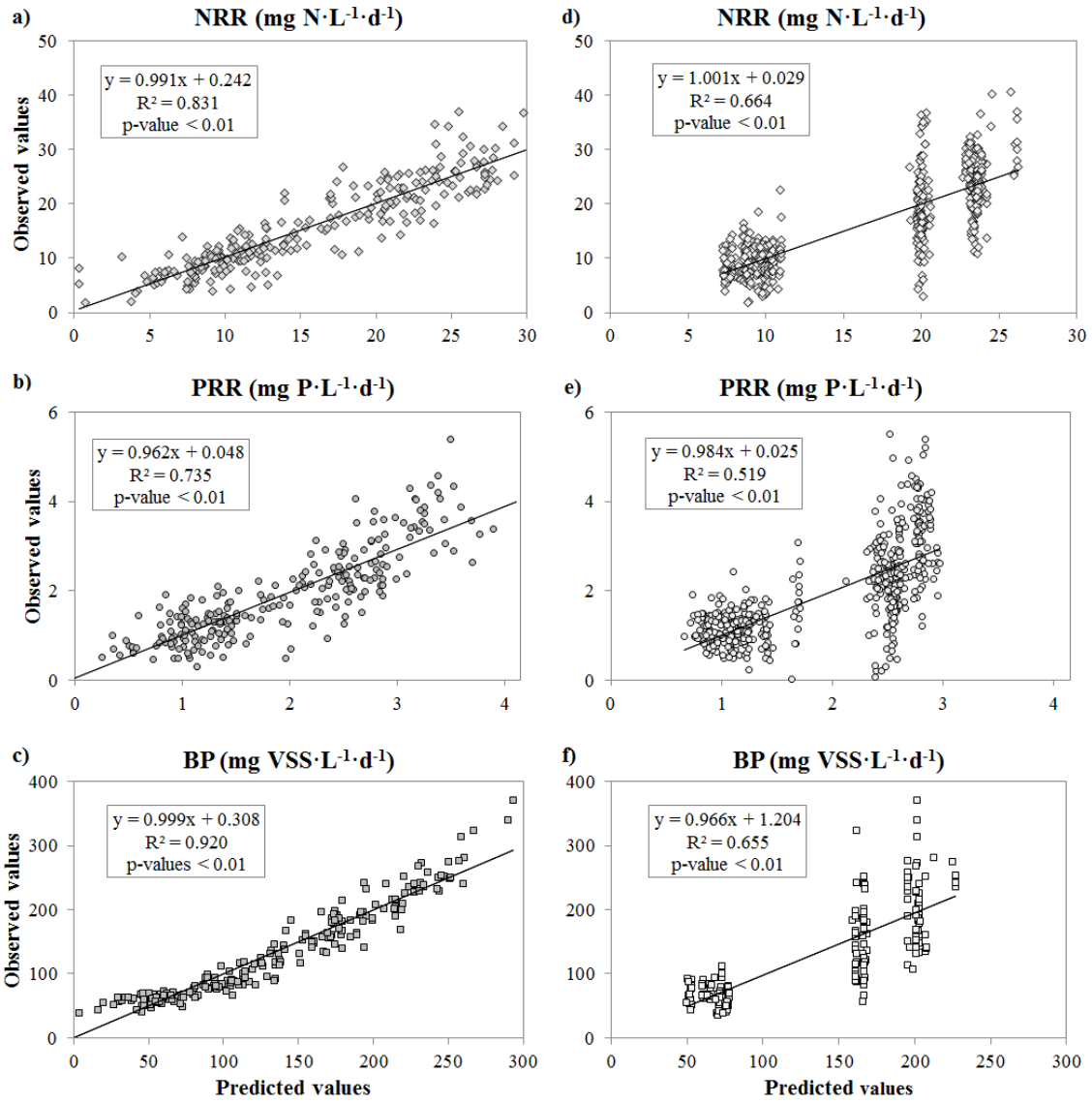

Figure 5.*Observed vs predicted values by the PLS model using all the variables as predictors:* ***a)*** *Nitrogen recovery rate (NRR****); b)*** *Phosphorus recovery rate (PRR) and,* ***c)*** *Biomass productivity (BP); observed vs predicted values by the PLS model that used only the controllable variables as predictors:* ***d)*** *NRR;* ***e)*** *PRR and,* ***f)*** *BP.*

To identify the most important variables in predicting MPBR microalgae performance, the variable importance of the PLS projection (VIP) is given in Figure 6b. The VIP parameter is a weighted summary of all the X-variable loadings of all the responses. As can be seen in Figure 6b, the two most important variables were air flow rate (F_{air}) and light path (Lp), which clearly proves that correct PBR design plays a key role in the process.

Air flow rate has been reported as a key parameter in culture mixing and liquid-gas mass transfer (Kubelka *et al.*, 2018). Mixing rate may also be related to the light integration of the reactor (Xu *et al.*, 2019). In fact, higher mixing rates make microalgae move rapidly from the lit parts of the reactor to darker zones, which improves biomass productivity (Barceló-Villalobos *et al.*, 2019). Light path is a key parameter in the light available to the reactor, since the radiated light decreases with depth due to the light absorbed by the water and biomass (Cho *et al.*, 2019).

Other important variables in MPBR performance were OD680, VSS, P, HRT, TEC, Chl, NH_4, N_t, NOxR and BRT (Figure 6b). In the loading plot (Figure 6a) all these variables were projected away from the plot origin, showing their important contribution to the PLS model. As can be seen in Figure 6a, the BRT and HRT operational parameters showed an inverse correlation pattern with MPBR performance (i.e. NRR, PRR and BP) since they were projected opposite to the plot origin. This was probably due to: i) shorter BRT and HRT tend to obtain higher MPBR performance until they reach an optimum value (Rada-Ariza *et al.*, 2019); ii) longer BRTs are likely to increase the shadow effect due to higher microalgae biomass and usually favour the proliferation of other microorganisms, reducing microalgae performance (González-Camejo *et al.*, 2019a); iii) longer HRT can limit microalgae due to nutrient depletion (Gao *et al*., 2018; González-Camejo *et al.*, 2018). When the system is nutrient-limited,

N_t, NH_4 and P can also have a significant effect in MPBR performance. In this respect, other authors have reported microalgae limitation when ammonium and phosphorus are under 10 and 1 $mg \cdot L^{-1}$, respectively (Pachés *et al.*, 2018). Since these effluent variables are also related to microalgae nutrient uptake, it is therefore reasonable to expect that P, NH_4 and N_t presented a relatively high inverse correlation with microalgae performance (Figure 6a).

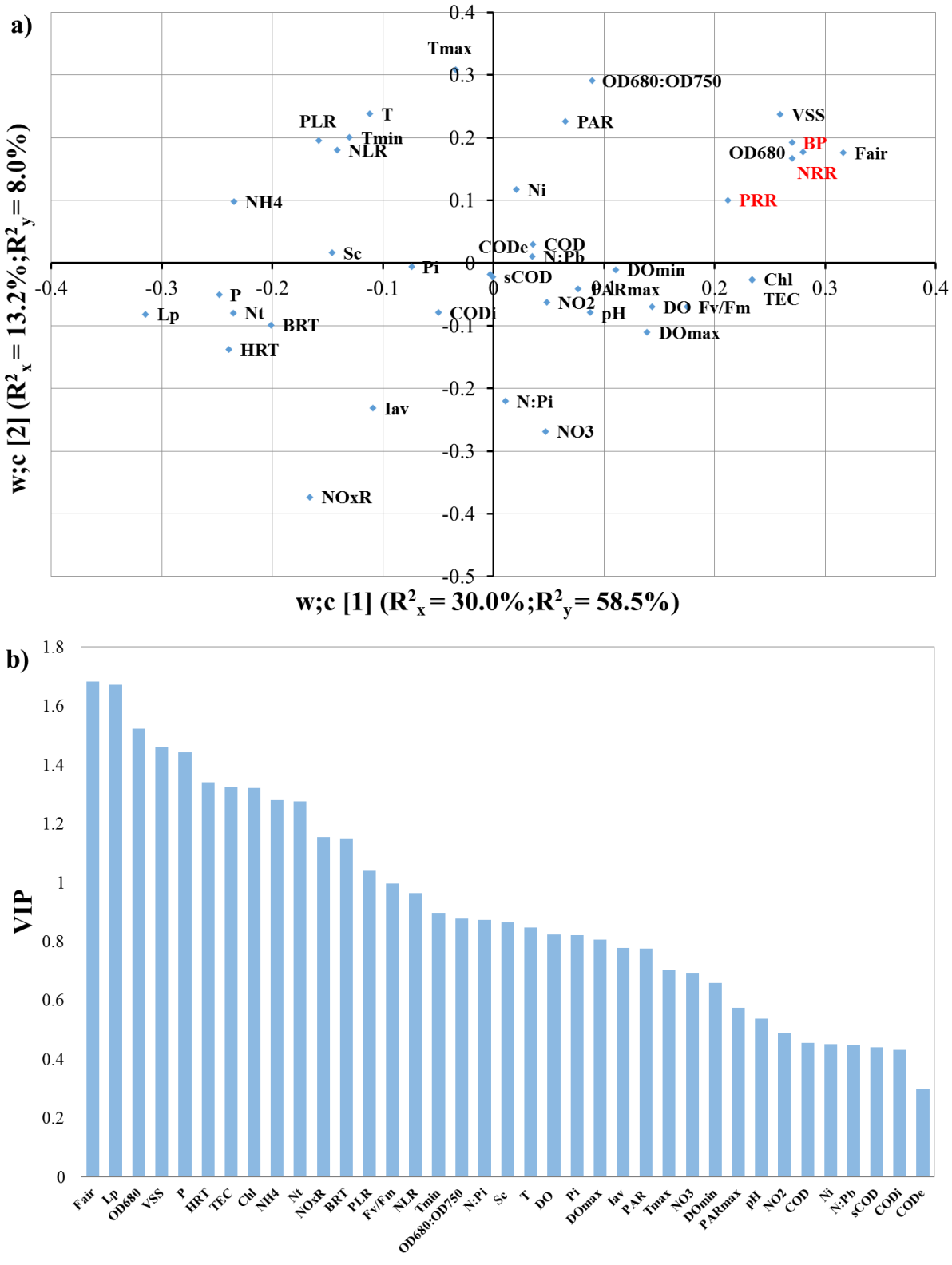

Figure 6. *Results of the fitted PLS model: a) Weight plot of the first two latent variables; b) Variable Importance in the projection (VIP) of the explicative variables.*

As expected, OD680 was highly correlated with biomass productivity since its correlation with VSS (which is inversely proportional to BP) was high (R^2 = 89.1%, Figure 4a). In addition, the culture was dominated by eukaryotic bacteria, as TEC was proportional to VSS (Figure 4b). TEC was thus also expected to be closely related to system performance, as was Chl concentration, since *Chlorella* was the main eukaryotic microalgae genus during most of the 3-year continuous operation (Figure 4d), as explained in Section 3.1.

Another important factor was the nitrification rate, which confirms that microalgae-AOB competition for ammonium uptake had significant effect on MPBR performance, as suggested by González-Camejo *et al.* (2019c). For this reason, another PLS analysis was carried out to consider NOxR as a response (see section 3.4).

Many other variables appeared to be correlated with MPBR performance, which agrees with Cho *et al.* (2019) and corroborates the difficulty of controlling outdoor microalgae cultivation. However, the PLS results highlight the fact that MPBR performance is more dependent on the operating and design parameters (such as light path, air flow rate, BRT and HRT) than on ambient conditions like solar PAR and temperature (Figure 6b). Light and temperature have been widely reported as key parameters in nutrient assimilation and microalgae growth (Galès *et al.*, 2019; Marazzi *et al.*, 2019). The limited influence of environmental factors in the PLS model of MPBR performance may be due to the fact that PAR and temperature represent the daily average value of these parameters. Solar radiation variation was around 50-500 $\mu mol \cdot m^{-2} \cdot s^{-1}$, while instant solar radiation varied in the range of 0-2000 $\mu mol \cdot m^{-2} \cdot s^{-1}$ (Galès *et al.*, 2019).

In addition, the MPBR plant was additionally lit from an artificial light source (Section 2.2) which provided better control of the light photons and reduced the shadow effect of the culture. Temperature can vary by more than 10 ºC throughout the day, although

temperatures over 30 ºC were avoided by cooling the culture (Section 2.2). All these factors reduced culture light and temperature variations and may have contributed to the small influence of ambient parameters on the PLS model.

COD_e, COD_i, COD, N_i, sCOD and NO_2 showed low correlations with microalgae performance (Figure 6b). Since COD_i came from an AnMBR plant which degraded most of the organic matter content (Seco *et al.*, 2018) and COD_e was the permeate of an ultrafiltration system which removed most of the suspended organic matter, their variability was relatively low, so that COD_e and COD_i concentrations were not expected to have a significant influence on the model. However, the culture's COD concentration was expected to have a stronger influence on the projection model, since the presence of organic carbon in the wastewater has been reported to be able to modify the microalgae cell metabolism, changing their activity (Moreno-García *et al.*, 2019). In addition, COD is usually directly related to microalgae biomass (Ambat *et al.* (2018)). sCOD concentration was also expected to show higher influence on MPBR performance as it can be used as an indirect measure of extracellular organic matter (EOM) content. However, the results of the fitted PLS model gave little weight to these variables (Figure 6b), possibly due to the production of these organic compounds being increased either to microalgae activity (Lau *et al*., 2019), or when algae are under stress (Lee *et al.*, 2018). In addition, the proliferation of competing organisms such as heterotrophs (which hinder microalgae activity) reduces the sCOD in the culture (Galès *et al.*, 2019). The variance in this parameter could thus be influenced by both high and low microalgae and heterotrophic bacteria activity and their correlation pattern could have changed throughout the 3-year operating period, reducing their importance in the overall model.

Unexpectedly, NO_2 showed a relatively small influence on the PLS model, since nitrite was found to inhibit microalgae growth (González-Camejo *et al.*, 2019b). However, nitrite concentration was negligible most of the time during MPBR operations, which means little variation in this parameter and so insignificant microalgae growth inhibition. This was probably the reason why this variable had little influence on the model.

3.3 Controllable variables

Of all the variables assessed in the PCA (Section 3.1) only Lp, F_{air}, HRT and BRT could be modified or controlled, since they were either design or operating parameters. The remainder were either values obtained from measurements or microalgae performance parameters and thus could not be modified as desired. Another PLS analysis was therefore performed considering only the controlled variables as predictors (X-matrix).

Figures 5d, 5e and 5f show the values obtained versus the predicted values by the new PLS model. In comparison to Figures 5a, 5b and 5c, it is evident that despite the new PLS model's moderately accurate prediction capacity for NRR, PRR and BP, its capacity was noticeably worse than the PLS with the full X-matrix as predictors. This highlights the variability of the data obtained in outdoor systems, as reported by Marazzi *et al.* (2019) and Xu *et al.* (2019) and confirms the influence of the influent, effluent, ambient and culture variables on MPBR performance. It can thus be concluded that the microalgae cultivation process can only be partially controlled by the design and operating variables, although there are other parameters related to ambient conditions (such as light and temperature), biotic (competition with other microorganisms) and abiotic factors (e.g. nutrient loads and pH) that also play a

significant role in microalgae cultivation (Ambat *et al.*, 2018; Barceló-Villalobos *et al.*, 2019; Galès *et al*., 2019; Qiu *et al.*, 2017).

3.4 Nitrification

In the cultivation system studied, the competition between microalgae and ammonium oxidising bacteria for ammonium uptake can play a key role in MPBR plant performance, as has been shown in González-Camejo *et al.* (2019c). If nitrifying bacteria activity is low, microalgae will be favoured (Marcilhac *et al*., 2014). Conditions that minimise nitrifying bacteria will thus be pursued. For this reason, a specific PLS analysis was carried out to determine the main variables related to nitrifying bacteria activity to obtain information on the prevalent conditions that affect growth.

The PLS was performed using the same predictors as those described in Section 3.2., but with the nitrification rate (NOxR) as the response. Four latent variables were statistically significant in the fitted PLS model, according to cross-validation. The model explained 56.2% of X-matrix variance (R^2_x) and 85.3% of the response variable (R^2_y), with a goodness of prediction parameter (Q^2) that reached 78.0%. The PLS model performance was good, as can be seen in the measured versus predicted PLS nitrification rate (see Figure 7a).

Figure 7b shows the VIP of all the explicative variables (X-matrix). As can be seen, the effluent nitrate concentration was the most important parameter related to NOxR variability. AOB compete with microalgae for ammonium uptake, transforming it into nitrite, while nitrite oxidising bacteria (NOB) carry out the second step of nitrification, oxidising nitrite to nitrate. If NOB activity is similar or higher than that of AOB, nitrite therefore does not accumulate and the concentration of NO_3 appears as a good indicator

of nitrifying bacteria activity (Galès *et al.*, 2019). It should be noted that despite microalgae being able to absorb nitrate to grow, its consumption rate is significantly lower than that of ammonium (González-Camejo *et al.*, 2019c). High NOxR is thus inadvisable to reach maximum microalgae performance.

NRR was another factor which explained high variability of the nitrification rate. In the loading plot of the first two latent variables of the fitted PLS model (Figure 7c), the projection of both variables lay in opposite quadrants, indicating an inverse correlation pattern between them. This result corroborates which was reported by González-Camejo *et al.* (2018; 2019c) and Rada-Ariza *et al.* (2019), who found that (in short-term periods) nitrification rates fell when microalgae activity was higher and highlights the importance of reducing nitrifying bacteria activity to the minimum to achieve maximum nitrogen recovery by microalgae.

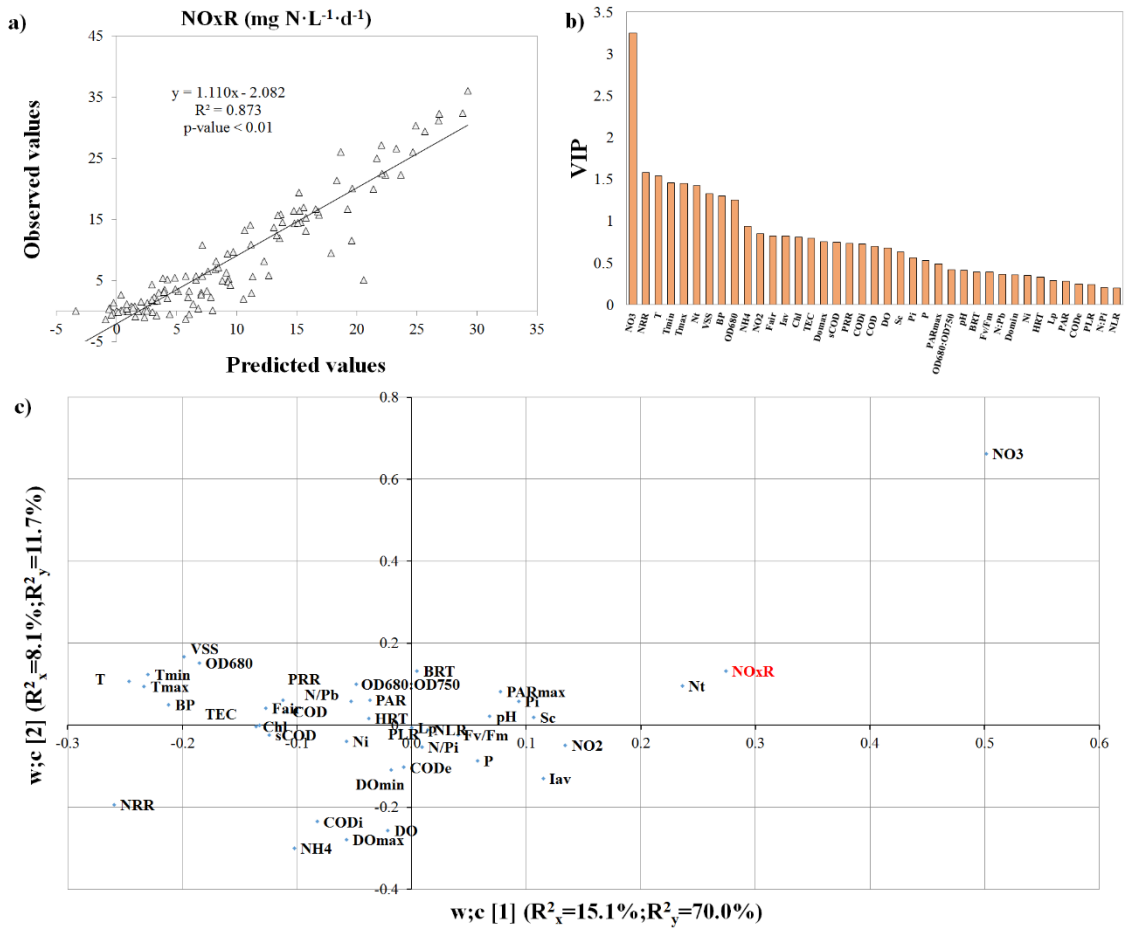

Figure 7. *PLS model to predict the nitrification rate (NOxR):* ***a)*** *Observed vs predicted values;* ***b)*** *Variable Importance in the projection (VIP) of the explicative variables; and* ***c)*** *Weight plot of the first two latent variables*

With respect to factors other than performance and effluent variables, the recorded parameters related to temperature (i.e., T, T_{min} and T_{max}) showed the highest correlation with NOxR (Figure 7b). This was probably due to the high influence of temperature on nitrifying bacteria activity. In fact, González-Camejo *et al.* (2019c) showed that AOB can dominate the competition at high temperatures, surpassing the microalgae. This means that keeping nitrifying bacteria at moderate temperatures seems to be the main control parameter to minimise nitrifying bacteria activity. After temperature, VSS and OD680 were the most relevant culture variables related to NOxR (Figure 7b). This was

probably related to the fact that higher microalgae biomass concentration (which was proportional to VSS and OD680, as can be seen in Figure 4) tended to favour microalgae activity in the competition with AOB for ammonium, as suggested by Rada-Ariza *et al.* (2019).

On the other hand, the influence of BRT was surprisingly lower than the other variables (Figure 7b). In this respect, Munz *et al.* (2011) observed partial nitrification (i.e., NO_2 accumulation) when BRT was under 2 days in an activated sludge reactor, while full nitrification (i.e., NO_3 production) was achieved at BRTs between 3-5 days. The study of the MPBR plant corresponding to nitrite inhibition (González-Camejo *et al.*, 2019b) showed the highest NRR and the lowest NOxR at a BRT of 2.5 days, while 2 and 4.5 days reduced MPBR performance (Table 1). It therefore seems that there was no linear correlation between BRT and NOxR.

4 Conclusions

Data obtained during the 3-year operation of an MPBR plant was analysed by statistical projection methods. Of the 40 variables evaluated, PCA indicated that the photobioreactor light path was the factor with the highest influence on data variability. Other relevant factors were F_{air}, NRR, PRR, BP, OD680, NH_4, P, HRT, BRT, NLR and PLR.

The parameters that explained the highest variability of microalgae performance were Lp, F_{air}, OD680, VSS, P, HRT, TEC, Chl, NH_4, N_t, NOxR and BRT. On the other hand, ambient factors (solar irradiance and temperature) showed a lower influence on MPBR performance.

The MPBR performance estimated by the PLS model worsened appreciably when only the controllable variables (Lp, F_{air}, HRT and BRT) were used as predictors, which

highlights the importance of other variables in MPBR performance, and shows that the microalgae cultivation process can only be partially controlled by the design and operating variables.

Temperature and microalgae biomass concentration appeared as leading parameters in controlling nitrification, while BRT had a relatively small influence on AOB activity.

Acknowledgments

This research work was supported by the Spanish Ministry of Economy and Competitiveness (MINECO, Projects CTM2014-54980-C2-1-R and CTM2014-54980-C2-2-R) jointly with the European Regional Development Fund (ERDF), both of which are gratefully acknowledged. It was also supported by the Spanish Ministry of Education, Culture and Sport via a pre-doctoral FPU fellowship to author J. González-Camejo (FPU14/05082).

References

1. Ambat, I., Tang, W.T., Sillanpaa, M., 2018. Statistical analysis of sustainable production of algal biomass from wastewater treatment process. Biomass and Bioenergy 120, 471–478. https://doi.org/10.1016/j.biombioe.2018.10.016
2. APHA-AWWA-WPCF, 2005. Standard methods for the examination of water and wastewater, 21nd edition. American Public Health Association, American Water Works Association, Water Pollution Control Federation. Washington DC, USA.
3. Arbib, Z., Ruiz, J., Álvarez-Díaz, P., Garrido-Pérez, C., Barragan, J., Perales, J.A., 2013. Long term outdoor operation of a tubular airlift pilot photobioreactor and a high rate algal pond as tertiary treatment of urban wastewater. Ecol. Eng., 52, 143-153. http://dx.doi.org/10.1016/j.ecoleng.2012.12.089

4. Barceló-Villalobos, M., Fernández-del Olmo, P., Guzmán, J.L., Fernández-Sevilla, J.M., Acién Fernández, F.G., 2019. Evaluation of photosynthetic light integration by microalgae in a pilot-scale raceway reactor, Bioresour. Technol. 280, 404-411. https://doi.org/10.1016/j.biortech.2019.02.032
5. Cho, K., Cho, D.H., Heo, J., Kim, U., Lee, Y.J., Choi, D.Y., Kim, H.S., 2019. Nitrogen modulation under chemostat cultivation mode induces biomass and lipid production by *Chlorella vulgaris* and reduces antenna pigment accumulation. Bioresour. Technol. 281, 118-125. https://doi.org/10.1016/j.biortech.2019.02.063
6. Galès, A., Bonnafous, A., Carré, C., Jauzein, V. Lanouguère, E., Le Floc'ha, E., Pinoit, J., Poullain, C., Roques, C., Sialve, B., Simier, M., Steyer, J.P., Fouilland, E., 2019. Importance of ecological interactions during wastewater treatment using High Rate Algal Ponds under different temperate climates, Algal Res. 40, 101508. https://doi.org/10.1016/j.algal.2019.101508
7. Gao, F., Penga, Y.Y., Lia, C., Cuia, W., Yang, Z.H., Zeng, G.M., 2018. Coupled nutrient removal from secondary effluent and algal biomass production in membrane photobioreactor (MPBR): Effect of HRT and long-term operation. Chem. Eng. J. 335, 169-175. http://dx.doi.org/10.1016/j.cej.2017.10.151
8. García, J., Ortiz, A., Álvarez, E., Belohlav, V., García-Galán, M.J., Díez-Montero, R., Álvarez, J.A., Uggetti, E., 2018. Nutrient removal from agricultural run-off in demonstrative full scale tubular photobioreactors for microalgae growth. Ecological Eng. 120, 513–521. https://doi.org/10.1016/j.ecoleng.2018.07.002
9. González-Camejo, J., Jiménez-Benítez, A., Ruano, M.V., Robles, A., Barat, R., Ferrer, J., 2019a. Optimising an outdoor membrane photobioreactor for tertiary

sewage treatment. J. Environ. Manag. 245, 76-85. https://doi.org/10.1016/j.jenvman.2019.05.010

10. González-Camejo, J., Montero, P., Aparicio, S., Ruano, M.V., Borrás, L., Barat, R., Ferrer, J., Seco, A., 2019b. Assessment of the nitrite inhibition of microalgae at bench and pilot scale. IWA Conference on Algal Technologies and Stabilization Ponds for Wastewater Treatment and Resource Recovery. IWAlgae2019. 1-2 July 2019. Valladolid, Spain.
11. González-Camejo, J., Aparicio, A., Ruano, M.V., Borrás, L., Barat, R., Ferrer, J., 2019c. Effect of ambient temperature variations on an indigenous microalgae-nitrifying bacteria culture dominated by *Chlorella*. Bioresour. Technol. 290, 121788. https://doi.org/10.1016/j.biortech.2019.121788
12. González-Camejo, J., Barat, R., Ruano, M.V., Seco, A., Ferrer, J., 2018. Outdoor flat-panel membrane photobioreactor to treat the effluent of an anaerobic membrane bioreactor. Influence of operating, design and environmental conditions. Water Sci. Technol. 78(1), 195-206. http://dx.doi.org/10.2166/wst.2018.259
13. Han, H., Zhu, S., Qiao, J., Guo, M., 2018. Data-driven intelligent monitoring system for key variables in wastewater treatment process. Chinese journal of chemical engineering, 26(10), 2093-2101. https://doi.org/10.1016/j.cjche.2018.03.027
14. Ippoliti, D., Gómez, C., Morales-Amaral, M.M., Pistocchi, R., Fernández-Sevilla, J.M., Acién, F.G., 2016. Modeling of photosynthesis and respiration rate for *Isochrysis galbana* (T-Iso) and its influence on the production of this strain. Bioresour. Technol. 203, 71–79. http://dx.doi.org/10.1016/j.biortech.2015.12.050

15. Kubelka, B.G., Roselet, F., Pinto, W.T., Abreu, P.C., 2018. The action of small bubbles in increasing light exposure and production of the marine microalga *Nannochloropsis oceanica* in massive culture systems, Algal Res. 35, 69-76. https://doi.org/10.1016/j.algal.2018.09.030
16. Lau, A.K.S., Bilad, M.R., Osman, N.B., Marbelia, L., Putra, Z.A., Nordin, N.A.H.M., Wirzal, M.D.H., Jaafar, J., Khan, A.L., 2019. Sequencing batch membrane photobioreactor for simultaneous cultivation of aquaculture feed and polishing of real secondary effluent. Journal of Water Process Engineering 29, 100779. https://doi.org/10.1016/j.jwpe.2019.100779
17. Lee, J.C., Baek, K., Kim, H.W., 2018. Semi-continuous operation and fouling characteristics of submerged membrane photobioreactor (SMPBR) for tertiary treatment of livestock wastewater. J. Clean. Prod. 180, 244-251. https://doi.org/10.1016/j.jclepro.2018.01.159
18. Ling, Y., Sun, L.P., Wang, S.Y., Lin, C.S.K., Sun, Z., Zhou, Z.G., 2019. Cultivation of oleaginous microalga *Scenedesmus obliquus* coupled with wastewater treatment for enhanced biomass and lipid production. Biochem. Eng. J. 148, 162–169. https://doi.org/10.1016/j.bej.2019.05.012
19. Marazzi, F., Bellucci, M., Rossi, S., Fornaroli, R., Ficara, E., Mezzanotte, V., 2019. Outdoor pilot trial integrating a sidestream microalgae process for the treatment of centrate under non optimal climate conditions. Algal Res. 39, 1014-30. https://doi.org/10.1016/j.algal.2019.101430
20. Marcilhac, C., Sialve B., Pourcher A.M., Ziebal C., Bernet N., Béline F., 2014. Digestate color and light intensity affect nutrient removal and competition phenomena in a microalgal-bacterial ecosystem. Water Res. 64, 278-287. http://dx.doi.org/10.1016/j.watres.2014.07.012

21. Markou, G., Dao, L.H.T., Muylaert, K., Beardall, J., 2017. Influence of different degrees of N limitation on photosystem II performance and heterogeneity of *Chlorella vulgaris*. Algal Res. 26, 84-92. http://dx.doi.org/10.1016/j.algal.2017.07.005
22. Moreno-García, L., Gariepy, y., Barnabe, s., Raghavan, g.s.v., 2019. Effect of environmental factors on the biomass and lipid production of microalgae grown in wastewaters. Algal Res. 41, 101521. https://doi.org/10.1016/j.algal.2019.101521
23. Munz, G., Lubello, C., Oleszkiewicz, J.A., 2011. Factors affecting the growth rates of ammonium and nitrite oxidizing bacteria. Chemosphere, 83(5), 720-725. https://doi.org/10.1016/j.chemosphere.2011.01.058
24. Nayak, M., Dhanarajan, G., Dineshkumar, R., Sen, R., 2018. Artificial intelligence driven process optimization for cleaner production of biomass with co-valorization of wastewater and flue gas in an algal biorefinery. J. Clean. Prod. 201, 1092-1100. https://doi.org/10.1016/j.jclepro.2018.08.048
25. Pachés, M., Martínez-Guijarro, R., González-Camejo, J., Seco, A., Barat, R., 2018. Selecting the most suitable microalgae species to treat the effluent from an anaerobic membrane bioreactor. Environ. Technol. (in press). https://doi.org/10.1080/09593330.2018.1496148
26. Powell, N., Shilton, A., Chisti, Y., Pratt, S., 2009. Towards a luxury uptake process via microalgae – Defining the polyphosphate dynamics. Water Res. 43, 4207-4213. https://doi:10.1016/j.watres.2009.06.011
27. Qiu, R., Gao, S., Lopez, P.A., Ogden, K.L., 2017. Effects of pH on cell growth, lipid production and CO_2 addition of microalgae *Chlorella sorokiniana*, Algal Res. 28, 192-199. http://dx.doi.org/10.1016/j.algal.2017.11.004

28. Rada-Ariza, A.M., Fredy, D., Lopez-Vazquez, C.M., Van der Steen, N.P., Lens, P.N.L., 2019. Ammonium removal mechanisms in a microalgal-bacterial sequencingbatch photobioreactor at different solids retention times. Algal Res. 39, 101468. https://doi.org/10.1016/j.algal.2019.101468

29. Robles, A., Ruano, M.V., Ribes, J., Ferrer, J., 2013. Factors that affect the permeability of commercial hollow-fibre membranes in a submerged anaerobic MBR (HF-SAnMBR) system. Water Res. 47, 1277-1288. http://dx.doi.org/10.1016/j.watres.2012.11.055

30. Romero-Villegas, G.I., Fiamengo, M., Acién-Fernández, F.G., Molina-Grima, E., 2018. Utilization of centrate for the outdoor production of marine microalgae at the pilot-scale in raceway photobioreactors, J. Environ. Manag. 228, 506–516. https://doi.org/10.1016/j.jenvman.2018.08.020

31. Seco, A., Aparicio, S., González-Camejo, J., Jiménez-Benítez, A., Mateo, O., Mora, J.F., Noriega-Hevia, G., Sanchis-Perucho, P., Serna-García, R., Zamorano-López, N., Giménez, J.B., Ruiz-Martinez, A., Aguado, D., Barat, R., Borrás, L., Bouzas, A., Martí, N., Pachés, M., Ribes, J., Robles, A., Ruano, M.V., Serralta, J. and Ferrer, J., 2018. Resource recovery from sulphate-rich sewage through an innovative anaerobic-based water resource recovery facility (WRRF). Water Sci. Technol. 78(9), 1925-1936. https://doi.org/10.2166/wst.2018.492

32. Song, X., Luo, W., Hai, F.I., Price, W.E., Guo, W., Ngo, H.H., Nghiem, L.D., 2018. Resource recovery from wastewater by anaerobic membrane bioreactors: Opportunities and challenges. Bioresour. Technol. 270, 669-677. https://doi.org/10.1016/j.biortech.2018.09.001

33. Viruela A., Robles A., Durán F., Ruano M.V., Barat R., Ferrer J., Seco A., 2018. Performance of an outdoor membrane photobioreactor for resource recovery from anaerobically treated sewage. J. Clean. Prod. 178, 665-674. https://doi.org/10.1016/j.jclepro.2017.12.223
34. Whitton, R., Le Mével, A., Pidou, M., Ometto, F., Villa, R., Jefferson, B., 2016. Influence of microalgal N and P composition on wastewater nutrient remediation. Water Res. 91, 371-378. https://doi.org/10.1016/j.watres.2015.12.054
35. Xu, X., Gu, X., Wang, Z., Shatner, W., Wang, Z., 2019. Progress, challenges and solutions of research on photosynthetic carbon sequestration efficiency of microalgae. Renew. Sust. Energy Rev. 110, 65–82. https://doi.org/10.1016/j.rser.2019.04.050